Chapter 8: The Clamped Zernike Radial Polynomials

8.1 Introduction

When conversing between the optical and mechanical worlds, it would be desirable to be able to compensate for image aberrations using the structural mode shapes of the membrane optic. Such compensation might be desirable as structural mode shapes are preferred energy states of the system, and translating the optical aberration into a mechanical mode shape may provide another means for controlling optical image compensation. To the optical engineer, wavefronts are measured using Zernike polynomials. To mechanical engineers, wavefronts are more aptly described using structural mode shapes.

The overall goal of this chapter is to demonstrate a novel set of polynomials for describing image aberrations. Each of these polynomials is zero at the membrane edge, consequently bridging the gap between the mechanical and optical worlds of the membrane lens. In the first portion of this chapter, we will review the orthonormal mode shapes of a clamped circular membrane. Then, we will introduce the Zernike polynomials, a complete set of polynomials that are traditionally used in the optical world to describe image aberrations. Having established both, we will next discuss the use of a uniform actuation pressure and boundary displacement to statically correct the image aberration. We will then develop a novel set of polynomials, the *clamped* Zernike radial polynomials, and show their advantage over the traditional Zernike polynomials. Finally, we will describe the Fourier expansion of the clamped Zernike polynomials using the basis formed by the orthonormal mode shapes of the circular membrane and demonstrate analytically how these shapes could be used to make a nearly 100% effective deformable membrane lens for adaptive optics. This chapter reflects collaborative work between the Air Force Research Lab Directed Energy Directorate (AFRL/DE) and Virginia Tech in the area of adaptive membrane optics.

8.2 Orthonormal Mode Shapes of a Clamped Circular Membrane

The mode shapes of a clamped circular membrane are given by the solution to Bessel's equation,

$$\frac{d^2R}{dr^2}+\frac{1}{r}\frac{dR}{dr}+\left(\beta^2-\frac{\mu^2}{r^2}\right)R=0\,, \tag{8.1}$$

where Equation 8.1 is the spatial portion of the partial differential equation governing the membrane's transverse dynamics. The solutions to Equation 8.1 are given by

$$\begin{aligned}
&\Psi_{0n}(r,\theta)=A_{0n}J_0(\beta_{0n}r) && n=1,2...\\
&\Psi_{mnc}(r,\theta)=A_{mnc}J_m(\beta_{mn}r)\cos(m\theta) && m,n=1,2...\\
&\Psi_{mns}(r,\theta)=A_{mns}J_m(\beta_{mn}r)\sin(m\theta) && m,n=1,2...
\end{aligned} \tag{8.2}$$

Equations 8.2 emphasize that the clamped circular membrane has symmetric mode shapes, $\Psi_{0n}(r,\theta)$, that are unique, whereas the asymmetric mode shapes, $\Psi_{mnc}(r,\theta)$ and $\Psi_{mns}(r,\theta)$, are degenerate.

Next, we wish to normalize the mode shapes given by Equations 8.2. First, we will normalize the symmetric mode shapes. Following the procedure as outlined by Meirovich (1997), we write:

$$\int_{\Omega}\rho\Psi_{0n}d\Omega=\int_0^{2\pi}\int_0^{a}\rho A^2{}_{0n}J_0^2(\beta_{0n}r)rdrd\theta=1\,. \tag{8.3}$$

Evaluating the integral and solving for the constant A_{0n} we get:

$$\int_0^{2\pi}\int_0^{a}\rho\,A_{0n}^2\,J_0^2(\beta_{0n}r)rdrd\theta=\pi\,\rho\,a^2\,A_{0n}^2J_1^2(\beta_{0n}a)=1\quad, \tag{8.4}$$

and

$$A_{0n} = \frac{1}{aJ_1(\beta_{0n}a)\sqrt{\pi\rho}}\ . \tag{8.5}$$

Following the same procedure for the asymmetric modes, we get:

$$\int_0^{2\pi}\int_0^a \rho A_{mnc}^2 J_m^2(\beta_{mn}r)\cos^2(m\theta)rdrd\theta = \frac{\pi}{2}\rho a^2 A_{mnc}^2 J_{m+1}^2(\beta_{mn}a) = 1, \tag{8.6}$$

thus giving us:

$$A_{mnc} = A_{mns} = \frac{\sqrt{2}}{aJ_{m+1}(\beta_{mn}a)\sqrt{\pi\rho}}. \tag{8.7}$$

Having found the constants given by Equations 8.5 and 8.7, we now have a set of orthogonal and normalized (hence, orthonormal) mode shapes. By orthonormal, it means that the mode shapes demonstrate the following property:

$$\int_\Omega \Psi_i \Psi_j d\Omega = \begin{cases} 1 & i = j \\ 0 & i \neq j \end{cases}. \tag{8.8}$$

This property will help simplify our analysis in subsequent sections.

8.3 Zernike Polynomials

Image aberrations are often defined by a set of orthogonal functions known as the Zernike polynomials. Zernike polynomials are named after their original creator, Frits Zernike (circa 1934), who devised a complete set of polynomials orthogonal over a unit circle to describe wavefront distortions. Each Zernike polynomial (except for the primary piston mode) has maximum amplitude of +1, minimum amplitude of -1, and an average over the surface of zero (Tyson, 2000).

The Zernike functions are used to define wavefront aberration by the relation:

$$Z(r,\theta) = \sum_{n=0}^{k}\sum_{m=0}^{n} A_{nm} R_n^{n-2m}(r) \begin{cases} \sin\big((n-2m)\theta\big), & n-2m > 0 \\ \quad or & \\ \cos\big((n-2m)\theta\big), & n-2m \le 0 \end{cases}, \qquad (8.9)$$

in which the coefficients A_{nm} are a measure of the magnitude of each aberration (usually stated in wavelengths of light). The radial polynomial appearing in Equation 8.9, $R_n^{n-2m}(r)$, is defined by:

$$R_n^{n-2m}(r) = \sum_{s=0}^{m} (-1)^s \frac{(n-s)!}{s!(m-s)!(n-m-s)!} r^{(n-2s)}. \qquad (8.10)$$

As stated by Malacara (1992), only positive values of *n-2s* in Equation 8.10 are included in the summation. Also, Equation 8.9 can be written as a function of just a single index, *k*. By letting

$$k = \frac{n(n+1)}{2} + m + 1 \quad , \qquad (8.11)$$

we can describe an image aberration as $Z_k(r,\theta)$, indicating that the image aberration includes all terms up to term *k*. For example,

$$Z_4(r,\theta) = 1 + r\sin\theta + r\cos\theta + r^2\sin 2\theta\,. \tag{8.12}$$

Table 8.1 describes the first nine Zernike polynomials. A plot of these Zernike shape functions can be found in Figure 8.1.

Table 8.1. Description of the first nine Zernike polynomials.

n	***m***	***k***	**Zernike Polynomial**	**Description**
0	0	1	1	Piston
1	0	2	$r\sin\theta$	Tilt about *x axis*
1	1	3	$r\cos\theta$	Tilt about *y axis*
2	0	4	$r^2\sin 2\theta$	Astigmatism
2	1	5	$2r^2 - 1$	Defocus
2	2	6	$r^2\cos 2\theta$	Astigmatism
3	0	7	$r^3\sin 3\theta$	Trefoil
3	1	8	$\left(3r^3 - 2r\right)\sin\theta$	Coma
3	2	9	$\left(3r^3 - 2r\right)\cos\theta$	Coma

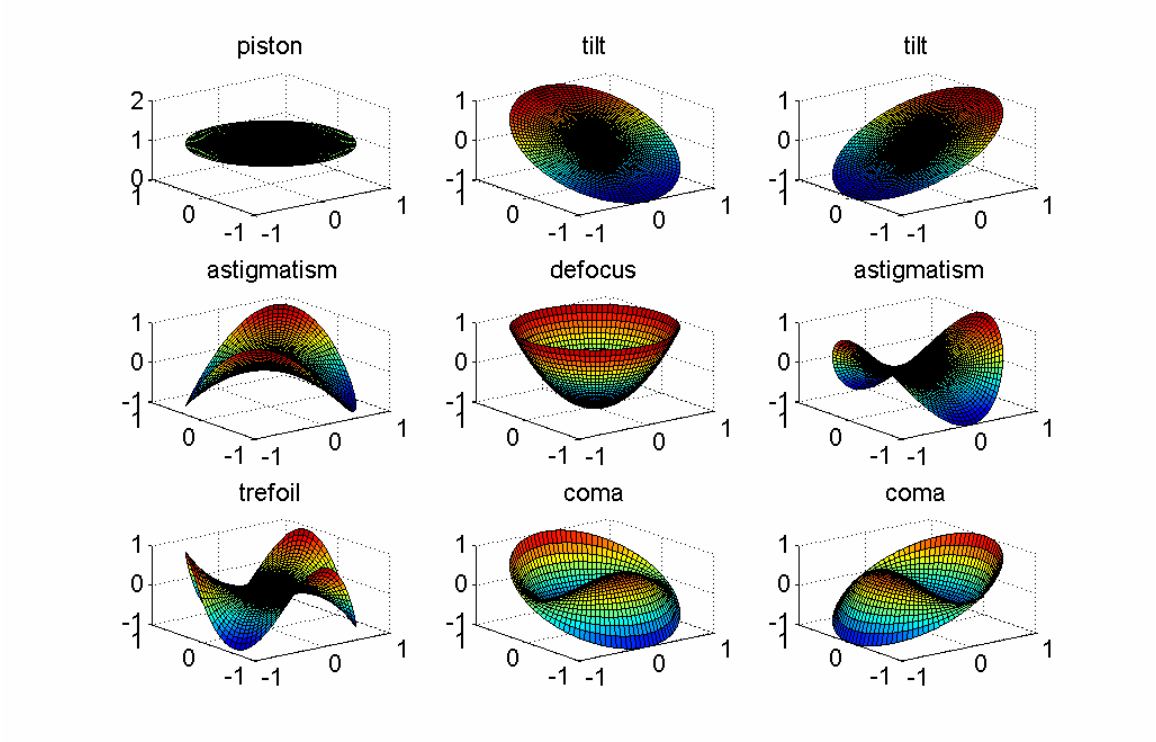

Figure 8.1. Sample plots of the Zernike polynomials describing particular wave front aberrations.

It is also important to point out that when the quantity *n-2m* is zero, the theta dependent portion of the Zernike polynomial drops out, leaving only a polynomial that is a function of the radius, *r*. The piston and defocus terms are examples of this rule (refer to Table 8.1). Further, when $m = 0$, the radial Zernike polynomials simplify to monomials of degree *n*, such that

$$R_n^n(r) = r^n . \tag{8.13}$$

We have now established the optical space and the modal space for a membrane lens. Next, we will look at using uniform pressure and boundary displacement to deform the surface of the membrane to correct for any image aberration. This original concept has been proposed by the AFRL/DE.

8.4 Static Image Aberration Compensation

To properly correct for image aberrations using a deformable mirror, geometrical optics suggests that the required displacement is half of the wavefront aberration (Malacara, 1992), namely:

$$w(\hat{r},\theta) = \frac{1}{2} Z(\hat{r},\theta). \tag{8.14}$$

Here, we introduce the non-dimensional variable $\hat{r} = \frac{r}{a}$, where a is the radius of the membrane lens.

As previously derived, the equation of motion governing the transverse dynamics of a circular membrane is given by

$$\nabla^2{}_{r\theta}\, w = \frac{1}{c^2} \frac{\partial^2 w}{\partial t^2}. \tag{8.15}$$

If a uniform pressure is acting on the interior surface of the membrane, then the difference between the top and bottom surface pressures, which we will denote as $\Delta p(r,\theta,t)$, enters into the equation of motion as a forcing function. Similarly, we can also assume for our analysis that a distributed, non-uniform pressure, $p_e(r,\theta,t)$, is able to act on the membrane. This non-uniform pressure may appear as an electrostatic pressure, and would be used to eliminate any remaining residual aberrations. The electrostatic pressure term, $p_e(r,\theta,t)$, enters the equation of motion in the same manner as the uniform pressure term. Assuming that the incoming wavefront aberrations are changing slowly enough for the membrane to achieve a new, static equilibrium position, then Equation 8.15 becomes

$$\nabla^2{}_{r\theta}\, w + \frac{\Delta p + p_e}{T} = 0, \tag{8.16}$$

where T is the applied tensile loading to the membrane. We can non-dimensionalize Equation 8.16 by introducing the variable $\hat{r}$ such that Equation 8.16 becomes

$$\nabla^2_{\hat{r}\theta} w = -\left(\frac{\Delta p + p_e}{T}\right)a^2, \tag{8.17}$$

where the Laplacian in dimensionless coordinates is given by

$$\nabla^2_{\hat{r}\theta} w = \frac{\partial^2 w}{\partial \hat{r}^2} + \frac{1}{\hat{r}}\frac{\partial w}{\partial \hat{r}} + \frac{1}{\hat{r}^2}\frac{\partial^2 w}{\partial \theta^2} = \frac{1}{\hat{r}}\frac{\partial}{\partial \hat{r}}\left(\hat{r}\frac{\partial w}{\partial \hat{r}}\right) + \frac{1}{\hat{r}^2}\frac{\partial^2 w}{\partial \theta^2}. \tag{8.18}$$

For the remainder of this chapter, we will assume that the measured image aberration consists of Zernike polynomials up to the 5th degree, so that we have

$$\begin{aligned} Z(\hat{r},\theta) = {} & A_{00} + A_{10}R_1^1(\hat{r})\cos\theta - A_{11}R_1^1(\hat{r})\sin\theta + A_{20}R_2^2(\hat{r})\cos(2\theta) + A_{21}R_2^0(\hat{r}) - A_{22}R_2^2(\hat{r})\sin 2\theta \\ & + A_{30}R_3^3(\hat{r})\cos 3\theta + A_{31}R_3^1(\hat{r})\cos\theta - A_{32}R_3^1(\hat{r})\sin\theta - A_{33}R_3^3(\hat{r})\sin 3\theta + A_{40}R_4^4(\hat{r})\cos 4\theta \\ & + A_{41}R_4^2(\hat{r})\cos 2\theta + A_{42}R_4^0(\hat{r}) - A_{43}R_4^2(\hat{r})\sin 2\theta - A_{44}R_4^4(\hat{r})\sin 4\theta \\ & + A_{50}R_5^5(\hat{r})\cos 5\theta + A_{51}R_5^3(\hat{r})\cos 3\theta + A_{52}R_5^1(\hat{r})\cos\theta - A_{53}R_5^1(\hat{r})\sin\theta \\ & - A_{54}R_5^3(\hat{r})\sin 3\theta - A_{55}R_5^5(\hat{r})\sin 5\theta. \end{aligned} \tag{8.19}$$

To help simplify our analysis, we substitute in the monomials (Equation 8.13) and the other radial polynomials (for example, see Table 13.1 in Malacara (1992)), as given by

$$\begin{aligned} & R_2^0 = 2\hat{r}^2 - 1, \quad R_4^0 = 6\hat{r}^4 - 6\hat{r}^2 + 1, \\ & R_3^1 = 3\hat{r}^3 - 2\hat{r}, \ R_4^2 = 4\hat{r}^4 - 3\hat{r}^2, \qquad , \\ & R_5^1 = 10\hat{r}^5 - 12\hat{r}^3 + 3\hat{r}, \ R_5^3 = 5\hat{r}^5 - 4\hat{r}^3 \end{aligned} \tag{8.20}$$

and can consequently rewrite Equation 8.19 as

$$
\begin{aligned}
Z(\hat{r},\theta) = {} & A_{00} + A_{10}\hat{r}\cos\theta - A_{11}\hat{r}\sin\theta + A_{20}\hat{r}^2\cos(2\theta) - A_{22}\hat{r}^2\sin 2\theta + A_{30}\hat{r}^3\cos 3\theta \\
& - A_{33}\hat{r}^3\sin 3\theta + A_{40}\hat{r}^4\cos 4\theta - A_{44}\hat{r}^4\sin 4\theta + A_{50}\hat{r}^5\cos 5\theta - A_{55}\hat{r}^5\sin 5\theta + A_{21}(2\hat{r}^2 - 1) \\
& + A_{42}(6\hat{r}^4 - 6\hat{r}^2 + 1) + (3\hat{r}^3 - 2\hat{r})(A_{31}\cos\theta - A_{32}\sin\theta) + (4\hat{r}^4 - 3\hat{r}^2)(A_{41}\cos 2\theta - A_{43}\sin 2\theta) \\
& + (10\hat{r}^5 - 12\hat{r}^3 + 3\hat{r})(A_{52}\cos\theta - A_{53}\sin\theta) + (5\hat{r}^5 - 4\hat{r}^3)(A_{51}\cos 3\theta - A_{54}\sin 3\theta).
\end{aligned}
\tag{8.21}
$$

Next, we collect like terms of the form $\hat{r}^n\cos n\theta$ and $\hat{r}^n\sin n\theta$ in Equation 8.21 and get

$$
\begin{aligned}
Z(\hat{r},\theta) = {} & A_{00} - A_{21} + A_{42} + (A_{10} - 2A_{31} + 3A_{52})\hat{r}\cos\theta - (A_{11} - 2A_{32} + 3A_{53})\hat{r}\sin\theta \\
& + (A_{20} - 3A_{41})\hat{r}^2\cos(2\theta) - (A_{22} - 3A_{43})\hat{r}^2\sin 2\theta + (A_{30} - 4A_{51})\hat{r}^3\cos 3\theta \\
& - (A_{33} - 4A_{54})\hat{r}^3\sin 3\theta + (A_{40})\hat{r}^4\cos 4\theta - (A_{44})\hat{r}^4\sin 4\theta + (A_{50})\hat{r}^5\cos 5\theta \\
& - (A_{55})\hat{r}^5\sin 5\theta + (2A_{21} - 6A_{42})\hat{r}^2 + 6A_{42}\hat{r}^4 + 3\hat{r}^3(A_{31}\cos\theta - A_{32}\sin\theta) \\
& + 4\hat{r}^4 A_{41}(\cos 2\theta - A_{43}\sin 2\theta) + (10\hat{r}^5 - 12\hat{r}^3)(A_{52}\cos\theta - A_{53}\sin\theta) \\
& + 5\hat{r}^5(A_{51}\cos 3\theta - A_{54}\sin 3\theta).
\end{aligned}
\tag{8.22}
$$

Combining Equation 8.14 and 8.17, we can solve for the required actuation pressure, namely,

$$
\Delta p + p_e = -\frac{T}{2a^2}\nabla^2 Z\,. \tag{8.23}
$$

To control the image aberration using just a uniform pressure and boundary displacement, we set $p_e(\hat{r},\theta,t) = 0$ in Equation 8.23. The general solution to Equation 8.17 has been solved by Wilkes (2005) and is given by:

$$
w_c(\hat{r},\theta) = C_0 + \left(\frac{a^2\Delta p}{4T}\right)(1-\hat{r}^2) + \sum_{n=1}^{\infty}\left(C_n\hat{r}_n\cos n\theta + D_n\hat{r}_n\sin n\theta\right), \tag{8.24}
$$

where C_0, C_n, and D_n are all constants to be determined based on the amount of aberration present in the measured wavefront signal. The correctable wavefront aberration, using the definition of Equation 8.14, is given by:

$$Z_c(\hat{r},\theta) = 2C_0 + 2\left(\frac{a^2\Delta p}{4T}\right)(1-\hat{r}^2) + 2\sum_{n=1}^{\infty}\left(C_n\hat{r}_n\cos n\theta + D_n\hat{r}_n\sin n\theta\right). \tag{8.25}$$

The residual aberration, $Z_{res}(\hat{r},\theta)$, is the difference between the measured aberration and the correctable portion, $Z_{res}(\hat{r},\theta) = Z(\hat{r},\theta) - Z_c(\hat{r},\theta)$. Explicitly, we have:

$$\begin{aligned}
Z_{res}(\hat{r},\theta) = {} & A_{00} - A_{21} + A_{42} + \left(A_{10} - 2A_{31} + 3A_{52}\right)\hat{r}\cos\theta - \left(A_{11} - 2A_{32} + 3A_{53}\right)\hat{r}\sin\theta \\
& + \left(A_{20} - 3A_{41}\right)\hat{r}^2\cos(2\theta) - \left(A_{22} - 3A_{43}\right)\hat{r}^2\sin 2\theta + \left(A_{30} - 4A_{51}\right)\hat{r}^3\cos 3\theta \\
& - \left(A_{33} - 4A_{54}\right)\hat{r}^3\sin 3\theta + \left(A_{40}\right)\hat{r}^4\cos 4\theta - \left(A_{44}\right)\hat{r}^4\sin 4\theta + \left(A_{50}\right)\hat{r}^5\cos 5\theta \\
& - \left(A_{55}\right)\hat{r}^5\sin 5\theta + \left(2A_{21} - 6A_{42}\right)\hat{r}^2 + 6A_{42}\hat{r}^4 + 3\hat{r}^3\left(A_{31}\cos\theta - A_{32}\sin\theta\right) \\
& + 4\hat{r}^4A_{41}\left(\cos 2\theta - A_{43}\sin 2\theta\right) + \left(10\hat{r}^5 - 12\hat{r}^3\right)\left(A_{52}\cos\theta - A_{53}\sin\theta\right) \\
& + 5\hat{r}^5\left(A_{51}\cos 3\theta - A_{54}\sin 3\theta\right) - 2\{C_0 + \left(\frac{a^2\Delta p}{4T}\right)(1-\hat{r}^2) + (C_1\hat{r}\cos\theta + D_1\hat{r}\sin\theta) \\
& + (C_2\hat{r}^2\cos 2\theta + D_2\hat{r}^2\sin 2\theta) + (C_3\hat{r}^3\cos 3\theta + D_3\hat{r}^3\sin 3\theta) \\
& + (C_4\hat{r}^4\cos 2\theta + D_4\hat{r}^4\sin 4\theta) + (C_5\hat{r}^5\cos 5\theta + D_5\hat{r}^5\sin 5\theta)\}.
\end{aligned} \tag{8.26}$$

By setting like power terms equal to each other, we see that the defocus terms (those proportional to $\hat{r}^2$) can be eliminated by applying a uniform pressure of

$$\Delta p = -\frac{4T}{a^2}\left(A_{21} - 3A_{42}\right). \tag{8.27}$$

Similarly, the piston (constant) term can be eliminated by rigidly displacing the boundary

$$C_0 = \frac{1}{2}\left(A_{00} + A_{21} - 5A_{42}\right). \tag{8.28}$$

Finally, solving for the remaining unknowns in Equation 8.26, we find that by displacing the boundary according to the following relations:

$$
\begin{aligned}
C_1 &= \frac{1}{2}\left(A_{10} - 2A_{31} + 3A_{52}\right), & D_1 &= -\frac{1}{2}\left(A_{11} - 2A_{32} + 3A_{53}\right), \\
C_2 &= \frac{1}{2}\left(A_{20} - 3A_{41}\right), & D_2 &= -\frac{1}{2}\left(A_{22} - 3A_{43}\right), \\
C_3 &= \frac{1}{2}\left(A_{30} - 4A_{51}\right), & D_3 &= -\frac{1}{2}\left(A_{33} - 4A_{54}\right), \\
C_4 &= \frac{1}{2}A_{40}, & D_4 &= -\frac{1}{2}A_{44}, \\
C_5 &= \frac{1}{2}A_{50}, & D_5 &= -\frac{1}{2}A_{55},
\end{aligned}
\tag{8.29}
$$

we can eliminate all terms of the form $\hat{r}^n \cos n\theta$ and $\hat{r}^n \sin n\theta$ for *n = 1, ..., 5*. The residual aberration (Equation 8.26) can therefore be reduced to

$$
\begin{aligned}
Z_{res}(\hat{r},\theta) = {} & 6A_{42}\hat{r}^4 + 3\hat{r}^3\left(A_{31}\cos\theta - A_{32}\sin\theta\right) + 4\hat{r}^4\left(A_{41}\cos 2\theta - A_{43}\sin 2\theta\right) \\
& + \left(10\hat{r}^5 - 12\hat{r}^3\right)\left(A_{52}\cos\theta - A_{53}\sin\theta\right) + 5\hat{r}^5\left(A_{51}\cos 3\theta - A_{54}\sin 3\theta\right).
\end{aligned}
\tag{8.30}
$$

A summary of the correctable aberrations and residual aberrations is given in Table 8.2. Notice that none of the residual aberration terms given in Table 8.2 are amiable to the boundary conditions imposed by the mechanical lens. Motivated by the inconsistencies between the mechanical and optical domains, the next section will derive a new basis with which to express the incoming image aberration. This new basis will be referred to as the *clamped* Zernike radial polynomials.

Table 8.2. Summary of wavefront correction for a membrane optic using uniform pressure difference (across the outer and inner surfaces of the membrane) and boundary displacement.

Zernike Polynomial	**Correctable Portion**	**Residual Aberration**
1	1	0
$\hat{r}\sin\theta$	$\hat{r}\sin\theta$	0
$\hat{r}\cos\theta$	$\hat{r}\cos\theta$	0
$\hat{r}^2\sin 2\theta$	$\hat{r}^2\sin 2\theta$	0
$2\hat{r}^2-1$	$2\hat{r}^2-1$	0
$\hat{r}^2\cos 2\theta$	$\hat{r}^2\cos 2\theta$	0
$\hat{r}^3\sin 3\theta$	$\hat{r}^3\sin 3\theta$	0
$\left(3\hat{r}^3-2\hat{r}\right)\sin\theta$	$-2\hat{r}\sin\theta$	$3\hat{r}^3\sin\theta$
$\left(3\hat{r}^3-2\hat{r}\right)\cos\theta$	$-2\hat{r}\cos\theta$	$3\hat{r}^3\cos\theta$
$\hat{r}^3\cos 3\theta$	$\hat{r}^3\cos 3\theta$	0
$\hat{r}^4\sin 4\theta$	$\hat{r}^4\sin 4\theta$	0
$\left(4\hat{r}^4-3\hat{r}^2\right)\sin 2\theta$	$-3\hat{r}^2\sin 2\theta$	$4\hat{r}^4\sin 2\theta$
$6\hat{r}^4-6\hat{r}^2+1$	$-6\hat{r}^2+1$	$6\hat{r}^4$
$\left(4\hat{r}^4-3\hat{r}^2\right)\cos 2\theta$	$-3\hat{r}^2\cos 2\theta$	$4\hat{r}^4\cos 2\theta$
$\hat{r}^4\cos 4\theta$	$\hat{r}^4\cos 4\theta$	0
$\hat{r}^5\sin 5\theta$	$\hat{r}^5\sin 5\theta$	0
$\left(5\hat{r}^5-4\hat{r}^3\right)\sin 3\theta$	$-4\hat{r}^3\sin 3\theta$	$5\hat{r}^5\sin 3\theta$
$\left(10\hat{r}^5-12\hat{r}^3+3\hat{r}\right)\sin\theta$	$3\hat{r}\sin\theta$	$\left(10\hat{r}^5-12\hat{r}^3\right)\sin\theta$
$\left(10\hat{r}^5-12\hat{r}^3+3\hat{r}\right)\cos\theta$	$\hat{r}\cos\theta$	$\left(10\hat{r}^5-12\hat{r}^3\right)\cos\theta$
$\left(5\hat{r}^5-4\hat{r}^3\right)\cos 3\theta$	$-4\hat{r}^3\cos 3\theta$	$5\hat{r}^5\cos 3\theta$
$\hat{r}^5\cos 5\theta$	$\hat{r}^5\cos 5\theta$	0

8.5 A Novel Transformation for Describing Image Aberrations

As previously mentioned, the mismatch between the mechanical and optical domains of the deformable membrane mirror poses a challenge. The following subsections will describe a novel basis with which to express the Zernike polynomials that is more suitable to the mechanical properties of the membrane lens.

First, we will define the *clamped* Zernike radial polynomials, and then we will apply this new set of polynomials to our static aberration correction analysis. A comparison between the residual aberrations from our previous analysis with the clamped Zernike radial polynomials analysis will demonstrate a significant advantage of using the newly proposed basis. Finally, we will look at possible methods of control based on the newly defined clamped residuals.

8.5.1 Definition of the Clamped Zernike Radial Polynomials

In this section, we will cast the wavefront aberration in terms of the dynamical mode shapes of a clamped circular membrane. In doing so, we will define a novel basis of *clamped* radial polynomials. Let us define the image aberration radial polynomial as:

$$R_n^{n-2m} \equiv R_n^{n-2m} - \hat{r}^{n-2m} + \hat{r}^{n-2m} \equiv C_n^{n-2m} + \hat{r}^{n-2m}, \tag{8.31}$$

where the clamped radial polynomials are defined as:

$$C_n^{n-2m} \equiv R_n^{n-2m}(\hat{r}) - \hat{r}^{n-2m}\ , \ m > 2\,, \tag{8.32}$$

which vanish at both $r = 0$ and at $r = 1$. This basis is advantageous to use as it has the same boundary conditions as the clamped membrane. This advantage will be exploited subsequently. Following the definition of Equation 8.32, we have

$$\begin{aligned} &C_4^0 = R_4^0 - \hat{r}^0 = 6\hat{r}^4 - 6\hat{r}^2, \\ &C_3^1 = R_3^1 - \hat{r}^1 = 3\hat{r}^3 - 3\hat{r}, \qquad C_4^2 = R_4^2 - \hat{r}^2 = 4\hat{r}^4 - 4\hat{r}^2, \\ &C_5^1 = R_5^1 - \hat{r}^1 = 10\hat{r}^5 - 12\hat{r}^3 + 2\hat{r}, \ C_5^3 = R_5^3 - \hat{r}^3 = 5\hat{r}^5 - 5\hat{r}^3. \end{aligned} \tag{8.33}$$

Next, we will insert our definition of the clamped Zernike radial polynomials into our measured wavefront aberration (Equation 8.19), thus yielding:

$$\begin{aligned}Z(\hat{r},\theta) = {} & A_{00} - A_{21} + A_{42} + (2A_{21})\hat{r}^2 + (A_{10} + A_{31} + A_{52})\hat{r}\cos\theta - (A_{11} + A_{32} + A_{53})\hat{r}\sin\theta \\ & + (A_{20} + A_{41})\hat{r}^2\cos(2\theta) - (A_{22} + A_{43})\hat{r}^2\sin 2\theta + (A_{30} + A_{51})\hat{r}^3\cos 3\theta \\ & - (A_{33} + A_{54})\hat{r}^3\sin 3\theta + (A_{40})\hat{r}^4\cos 4\theta - (A_{44})\hat{r}^4\sin 4\theta + (A_{50})\hat{r}^5\cos 5\theta \\ & - (A_{55})\hat{r}^5\sin 5\theta + A_{42}C_4^0(\hat{r}) + A_{31}C_3^1(\hat{r})\cos\theta - A_{32}C_3^1(\hat{r})\sin\theta + A_{41}C_4^2(\hat{r})\cos 2\theta \\ & - A_{43}C_4^2(\hat{r})\sin 2\theta + A_{51}C_5^3(\hat{r})\cos 3\theta + A_{52}C_5^1(\hat{r})\cos\theta - A_{53}C_5^1(\hat{r})\sin\theta \\ & - A_{54}C_5^3(\hat{r})\sin 3\theta.\end{aligned} \tag{8.34}$$

Now, we wish to derive an expression for the residual wavefront error, as we previously defined in Equations 8.25 and 8.26. Performing a similar analysis as was performed by Wilkes (2005), we get the following expression:

$$\begin{aligned}Z_{res}(\hat{r},\theta) = {} & A_{00} - A_{21} + A_{42} + (2A_{21})\hat{r}^2 + (A_{10} + A_{31} + A_{52})\hat{r}\cos\theta - (A_{11} + A_{32} + A_{53})\hat{r}\sin\theta \\ & + (A_{20} + A_{41})\hat{r}^2\cos(2\theta) - (A_{22} + A_{43})\hat{r}^2\sin 2\theta + (A_{30} + A_{51})\hat{r}^3\cos 3\theta \\ & - (A_{33} + A_{54})\hat{r}^3\sin 3\theta + (A_{40})\hat{r}^4\cos 4\theta - (A_{44})\hat{r}^4\sin 4\theta + (A_{50})\hat{r}^5\cos 5\theta \\ & - (A_{55})\hat{r}^5\sin 5\theta + A_{42}C_4^0(\hat{r}) + A_{31}C_3^1(\hat{r})\cos\theta - A_{32}C_3^1(\hat{r})\sin\theta + A_{41}C_4^2(\hat{r})\cos 2\theta \\ & - A_{43}C_4^2(\hat{r})\sin 2\theta + A_{51}C_5^3(\hat{r})\cos 3\theta + A_{52}C_5^1(\hat{r})\cos\theta - A_{53}C_5^1(\hat{r})\sin\theta \\ & - A_{54}C_5^3(\hat{r})\sin 3\theta - 2\{C_0 + \left(\frac{a^2\Delta p}{4T}\right)(1-\hat{r}^2) + (C_1\hat{r}\cos\theta + D_1\hat{r}\sin\theta) \\ & + (C_2\hat{r}^2\cos 2\theta + D_2\hat{r}^2\sin 2\theta) + (C_3\hat{r}^3\cos 3\theta + D_3\hat{r}^3\sin 3\theta) \\ & + (C_4\hat{r}^4\cos 2\theta + D_4\hat{r}^4\sin 4\theta) + (C_5\hat{r}^5\cos 5\theta + D_5\hat{r}^5\sin 5\theta)\}.\end{aligned} \tag{8.35}$$

As before, we see that by setting like power terms equal to each other, the defocus terms (those proportional to $\hat{r}^2$) can be eliminated by applying a uniform pressure of

$$\Delta p = -\frac{4T}{a^2}A_{21}. \tag{8.36}$$

Similarly, the piston (constant) term can be eliminated by rigidly displacing the boundary

$$C_0 = \frac{1}{2}\left(A_{00} + A_{21} + A_{42}\right). \tag{8.37}$$

Finally, solving for the remaining unknowns in Equation 8.35, we find that by displacing the boundary according to the following relations:

$$\begin{aligned}
C_1 &= \frac{1}{2}\left(A_{10} + A_{31} + A_{52}\right), & D_1 &= -\frac{1}{2}\left(A_{11} + A_{32} + A_{53}\right), \\
C_2 &= \frac{1}{2}\left(A_{20} + A_{41}\right), & D_2 &= -\frac{1}{2}\left(A_{22} + A_{43}\right), \\
C_3 &= \frac{1}{2}\left(A_{30} + A_{51}\right), & D_3 &= -\frac{1}{2}\left(A_{33} + A_{54}\right), \\
C_4 &= \frac{1}{2}A_{40}, & D_4 &= -\frac{1}{2}A_{44}, \\
C_5 &= \frac{1}{2}A_{50}, & D_5 &= -\frac{1}{2}A_{55},
\end{aligned} \tag{8.38}$$

we can eliminate all terms of the form $\hat{r}^n \cos n\theta$ and $\hat{r}^n \sin n\theta$ for $n = 1, \ldots, 5$. The residual aberration (Equation 8.35) can therefore be reduced to

$$\begin{aligned}
Z_{res}(\hat{r},\theta) = {} & A_{42}C_4^0(\hat{r}) + A_{31}C_3^1(\hat{r})\cos(\theta) - A_{32}C_3^1(\hat{r})\sin\theta + A_{41}C_4^2(\hat{r})\cos 2\theta \\
& - A_{43}C_4^2(\hat{r})\sin 2\theta + A_{51}C_5^3(\hat{r})\cos 3\theta + A_{52}C_5^1(\hat{r})\cos\theta - A_{53}C_5^1(\hat{r})\sin\theta \\
& - A_{54}C_5^3(\hat{r})\sin 3\theta.
\end{aligned} \tag{8.39}$$

Due to our definition of the novel clamped Zernike radial polynomials, the residual aberration is proportional to the mode shapes of a clamped circular membrane. Table 8.3 summarizes the residuals from the previous traditional Zernike analysis as well as the current clamped Zernike analysis.

Table 8.3. Summary of the residual wavefront aberrations using only uniform pressure and boundary control as expressed using traditional Zernike radial polynomials and the proposed clamped Zernike radial polynomials.

Zernike Polynomial	Residual Aberration Traditional Zernike Radial	Residual Aberration Clamped Zernike Radial
$\left(3\hat{r}^3 - 2\hat{r}\right)\sin\theta$	$3\hat{r}^3 \sin\theta$	$3\left(\hat{r}^3 - \hat{r}\right)\sin\theta$
$\left(3\hat{r}^3 - 2\hat{r}\right)\cos\theta$	$3\hat{r}^3 \cos\theta$	$3\left(\hat{r}^3 - \hat{r}\right)\cos\theta$
$\left(4\hat{r}^4 - 3\hat{r}^2\right)\sin 2\theta$	$4\hat{r}^4 \sin 2\theta$	$4\left(\hat{r}^4 - \hat{r}^2\right)\sin 2\theta$
$6\hat{r}^4 - 6\hat{r}^2 + 1$	$6\hat{r}^4$	$6\left(\hat{r}^4 - \hat{r}^2\right)$
$\left(4\hat{r}^4 - 3\hat{r}^2\right)\cos 2\theta$	$4\hat{r}^4 \cos 2\theta$	$4\left(\hat{r}^4 - \hat{r}^2\right)\cos 2\theta$
$\left(5\hat{r}^5 - 4\hat{r}^3\right)\sin 3\theta$	$5\hat{r}^5 \sin 3\theta$	$5\left(\hat{r}^5 - \hat{r}^3\right)\sin 3\theta$
$\left(10\hat{r}^5 - 12\hat{r}^3 + 3\hat{r}\right)\sin\theta$	$\left(10\hat{r}^5 - 12\hat{r}^3\right)\sin\theta$	$\left(10\hat{r}^5 - 12\hat{r}^3 + 2\hat{r}\right)\sin\theta$
$\left(10\hat{r}^5 - 12\hat{r}^3 + 3\hat{r}\right)\cos\theta$	$\left(10\hat{r}^5 - 12\hat{r}^3\right)\cos\theta$	$\left(10\hat{r}^5 - 12\hat{r}^3 + 2\hat{r}\right)\cos\theta$
$\left(5\hat{r}^5 - 4\hat{r}^3\right)\cos 3\theta$	$5\hat{r}^5 \cos 3\theta$	$5\left(\hat{r}^5 - \hat{r}^3\right)\cos 3\theta$

To highlight the benefit of the proposed clamped Zernike radial expressions, Figures 8.2 – 8.5 plot the two residual expressions against each other. In the comparison plots, the sine and cosine terms have been set to unity, plotting the 2-D slice of each residual term along its angular line of maximum amplitude.

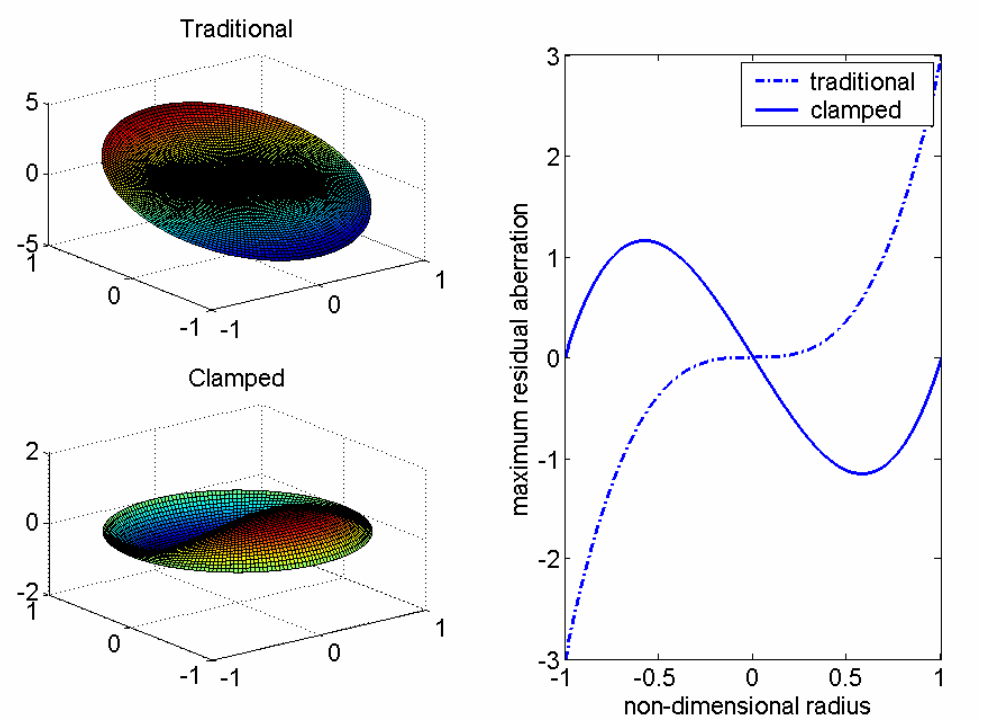

Figure 8.2. Comparison between the clamped Zernike polynomial residual $C_3^1(\hat{r})$ and the corresponding traditional Zernike residual.

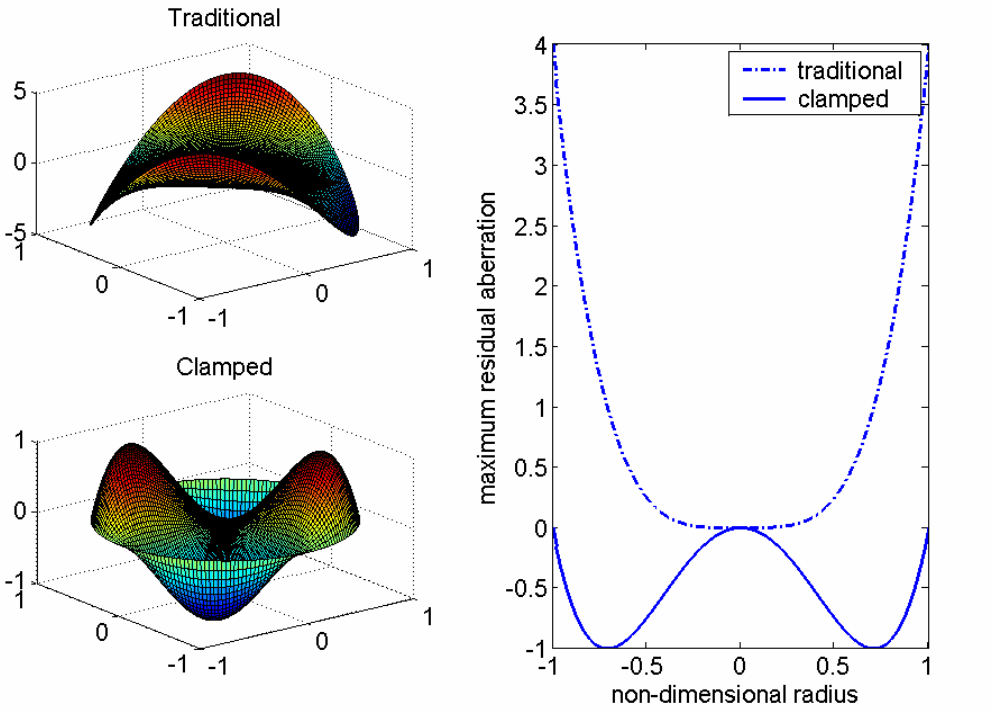

Figure 8.3. Comparison between the clamped Zernike polynomial residual $C_4^2(\hat{r})$ and the corresponding traditional Zernike residual.

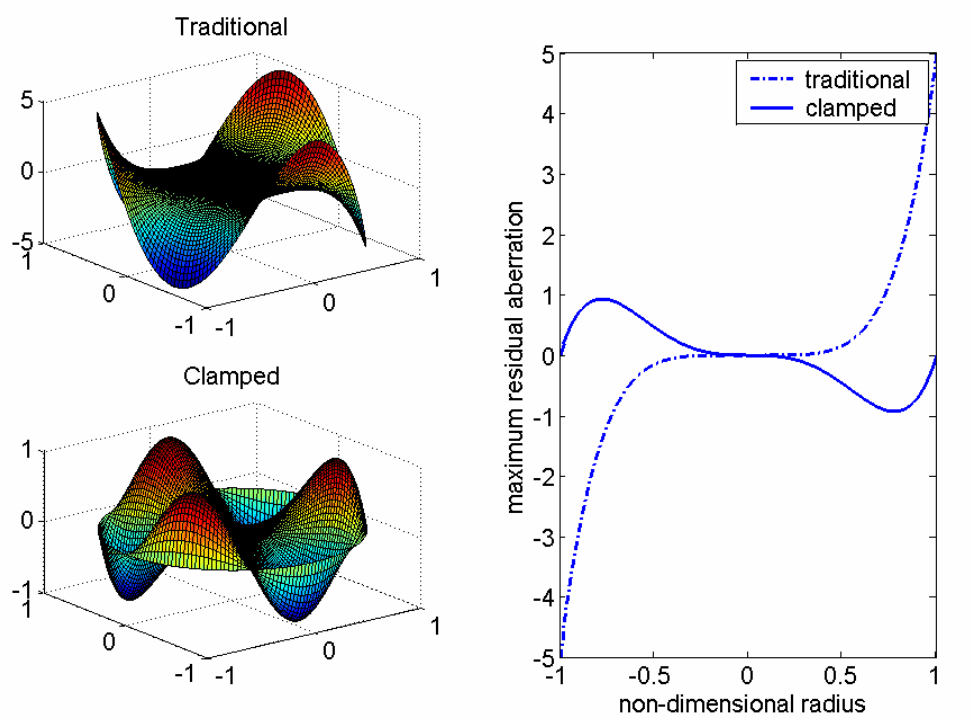

Figure 8.4. Comparison between the clamped Zernike polynomial residual $C_5^3(\hat{r})$ and the corresponding traditional Zernike residual.

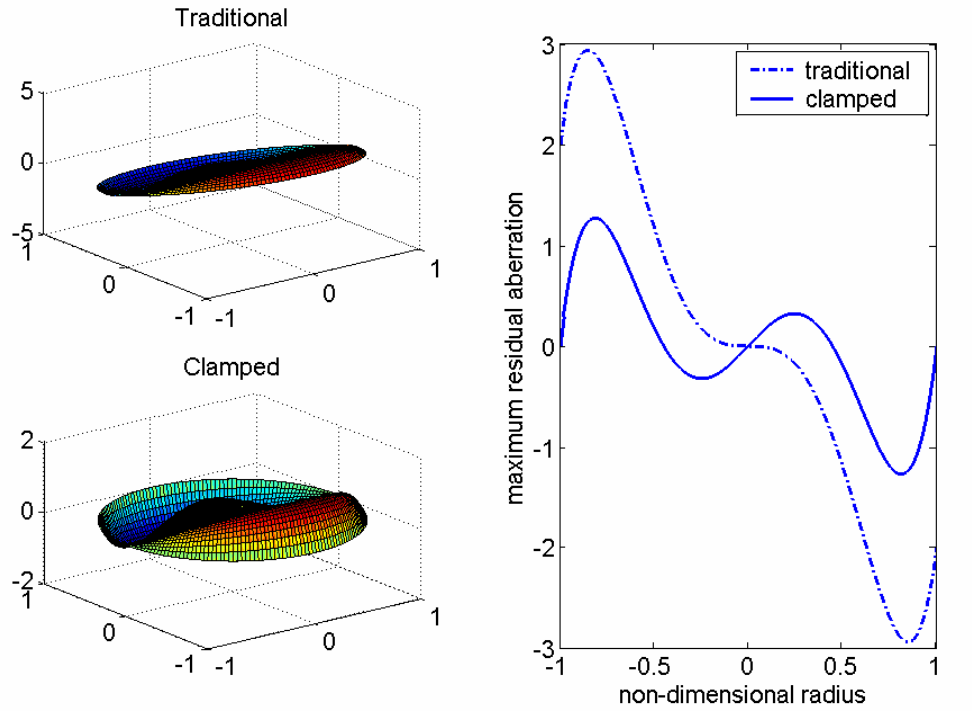

Figure 8.5. Comparison between the clamped Zernike polynomial residual $C_5^1(\hat{r})$ and the corresponding traditional Zernike residual.

8.5.2 Fourier Analysis of the Clamped Zernike Radial Polynomials

Up until this point in our analysis, we have assumed that only a uniform pressure and boundary control were available for image compensation control. Now we will relax this assumption and express the optically clamped Zernike radial polynomials in the mechanical domain of the membrane lens.

Given the clamped Zernike radial polynomials, denoted C_n^{n-2m}, describing the residual wavefront aberration, we wish to find the Fourier expansion approximation of the clamped Zernike shape functions using the basis formed by the mode shapes of a clamped circular membrane, denoted Ψ. Our Fourier expansion begins by assuming that, given the orthonormal basis formed by the mode shapes ψ_n and the functions C_n^{n-2m} living in the same Hilbert space, the function C_n^{n-2m} can be expressed as the Fourier series:

$$C_n^{n-2m} = z_0\psi_0 + z_1\psi_1 + z_2\psi_2 + \ldots + z_i\psi_i + \ldots . \tag{8.40}$$

We wish to find the constants z_n, otherwise known as the Fourier coefficients of C_n^{n-2m} with respect to the basis Ψ (Tolstov, 1962). To calculate the Fourier coefficients, we multiply Equation 8.40 by ψ_n and assume that the resulting series can be integrated term by term over the entire membrane domain, Ω. Doing so, we have:

$$\int_\Omega C_n^{n-2m}\psi_i d\Omega = z_i \int_\Omega \psi_i^2 d\Omega \quad (i = 1,2,\ldots) . \tag{8.41}$$

Solving for the Fourier coefficients, we get:

$$z_i = \frac{\int_\Omega C_n^{n-2m}\psi_i d\Omega}{\int_\Omega \psi_i^2 d\Omega} = \frac{\int_\Omega C_n^{n-2m}\psi_i d\Omega}{\left\| \psi_i^2 \right\|} . \tag{8.42}$$

Equations 8.40-8.42 assume equality, but such equality can only hold if an infinite number of basis functions are available. Since we do not have an infinite number of basis functions available, we will have to truncate our analysis and form the best approximation we can using a limited number of terms. We define the approximated clamped Zernike residual wavefront aberration as

$$C^N = z_0\psi_0 + z_1\psi_1 + z_2\psi_2 + ... + z_N\psi_N . \tag{8.43}$$

Further, note that since our basis Ψ was defined to be orthonormal previously, the norm appearing in Equation 8.42 is equal to unity. Substituting accordingly, we find that

$$z_i = \int_{\Omega} C_n^{n-2m}\psi_i d\Omega . \tag{8.44}$$

8.5.3 Example Fourier Expansion of the Clamped Zernike Radial Polynomials

Having defined our Fourier coefficients in Equation 8.44, we will now apply this expansion to the residual aberrations described using the clamped Zernike radial polynomials, as given explicitly in Table 8.3. We will form our modal basis from the first 36 mode shapes of the clamped membrane, including both symmetric and asymmetric modes. Further, we will only take the theta dependent mode shapes that are functions of sine and use them as a basis for the clamped Zernike radial polynomials that are also a function of sine and / or $\hat{r}$. We could also take the cosine terms in our analysis, but since they are orthogonal to the clamped Zernike radial polynomials, the integration term by term would give trivial solutions.

Now we will focus our analysis on the following residual aberration terms: $C_4^0, C_3^1\sin\theta, C_4^2\sin 2\theta, C_5^1\sin\theta,$ and $C_5^3\sin 3\theta$. Following through with the integration scheme stated in Equation 8.44 we get the following non-trivial terms:

$$
\begin{aligned}
C_4^0 \approx\ & -1.4276\psi_{01} - 1.2518\psi_{02} - 0.3659\psi_{03} - 0.1497\psi_{04} - 0.0748\psi_{05} - 0.0425\psi_{06}, \\
C_3^1 \sin\theta \approx\ & -1.0694\psi_{11s} - 0.1742\psi_{12s} - 0.0571\psi_{13s} - 0.0254\psi_{14s} - 0.0135\psi_{15s} - 0.0080\psi_{16s}, \\
C_4^2 \sin 2\theta \approx & -0.8883\psi_{21s} - 0.2017\psi_{22s} - 0.0767\psi_{23s} - 0.0372\psi_{24s} - 0.0208\psi_{25s} - 0.0128\psi_{26s}, \\
C_5^3 \sin 3\theta \approx & -0.7721\psi_{31s} - 0.2156\psi_{32s} - 0.0910\psi_{33s} - 0.0470\psi_{34s} - 0.0274\psi_{35s} - 0.0174\psi_{36s}, \\
C_5^1 \sin\theta \approx\ & -0.5894\psi_{11s} - 0.7622\psi_{12s} - 0.2986\psi_{13s} - 0.1411\psi_{14s} \ldots \\
& \qquad - 0.0768\psi_{15s} - 0.0462\psi_{16s} - 0.0002\psi_{56s}.
\end{aligned}
\tag{8.45}
$$

To further exhibit the excellent match between the modal expansion and the original residual aberration, Figures 8.6 – 8.10 plot the original residual, the projected residual, and the error between the two. In each of the plots, the residual aberrations have been normalized by their largest respective magnitude.

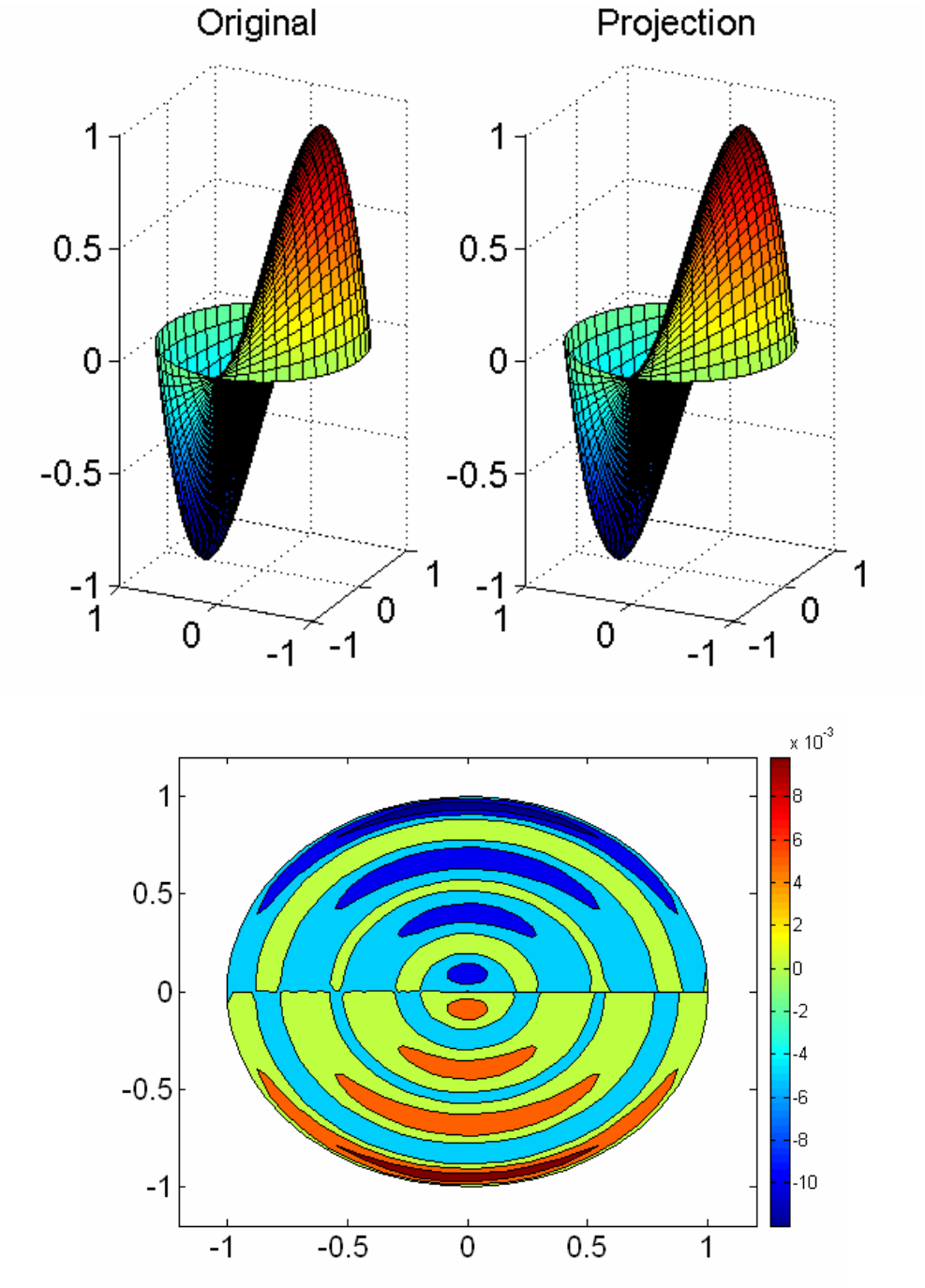

Figure 8.6. Comparison between the $C_3^1 \sin\theta$ residual term (top left) and its modal projection (top right) and the error between the two spaces (bottom).

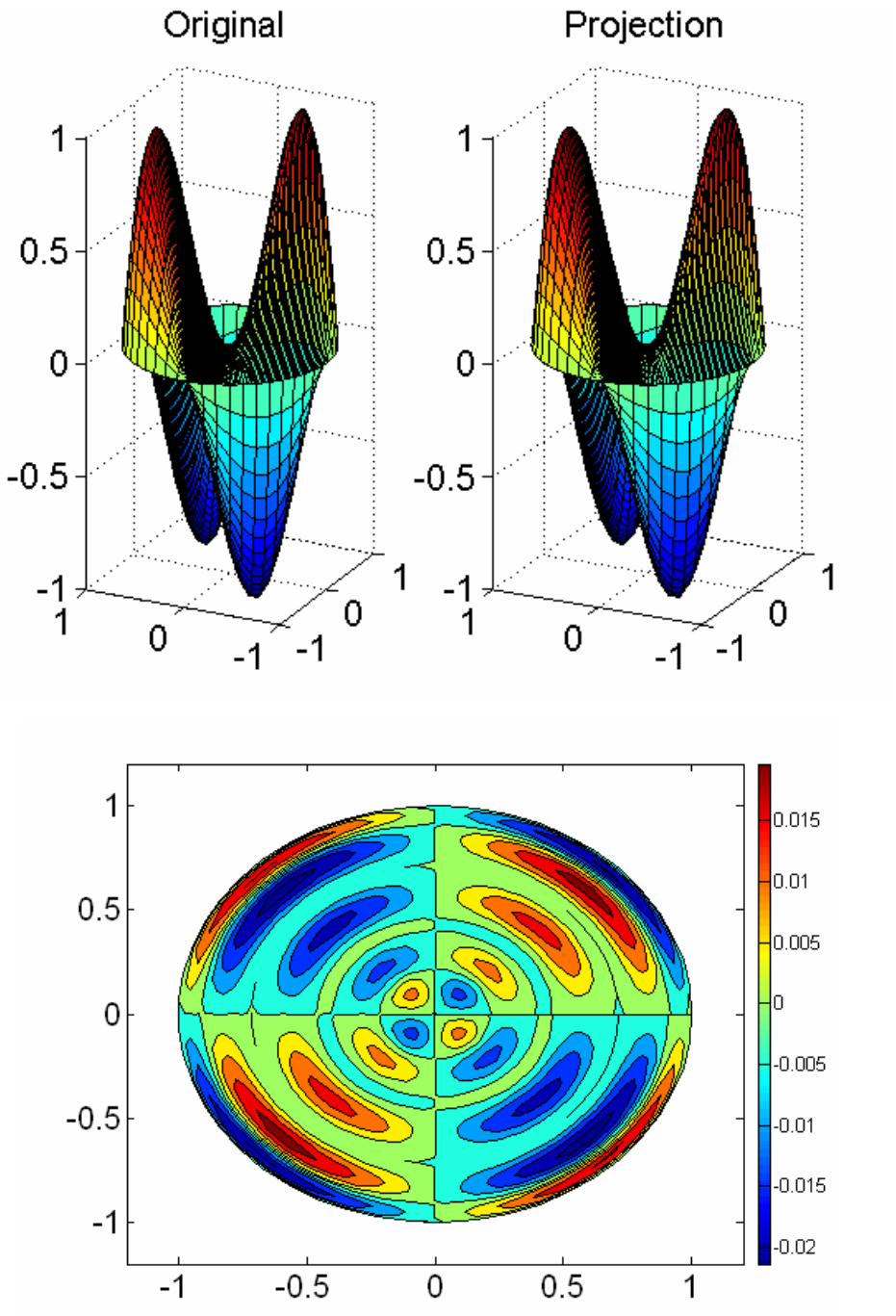

Figure 8.7. Comparison between the $C_4^2 \sin 2\theta$ residual term (top left) and its modal projection (top right) and the error between the two spaces (bottom).

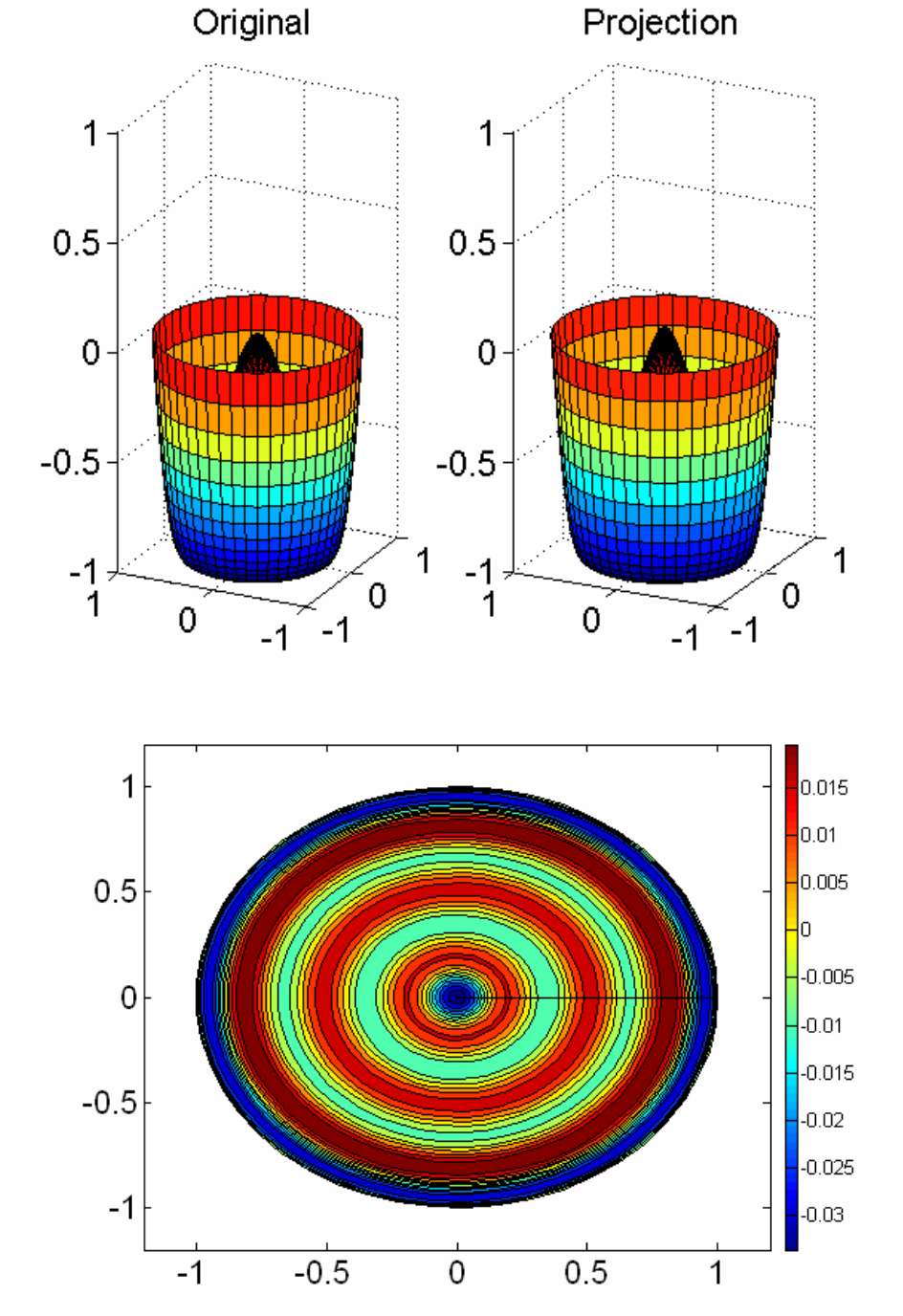

Figure 8.8. Comparison between the C_4^0 residual term (top left) and its modal projection (top right) and the error between the two spaces (bottom).

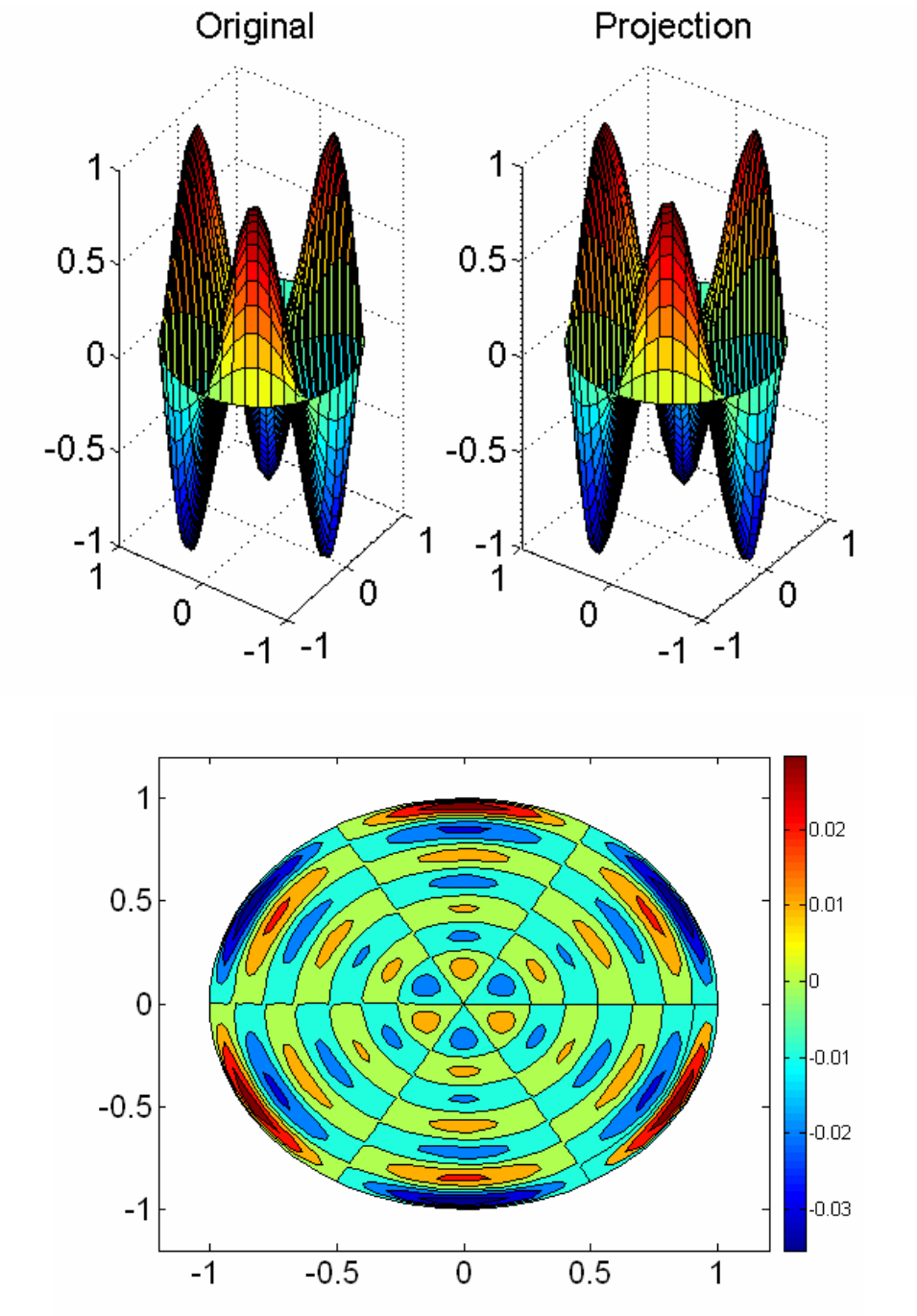

Figure 8.9. Comparison between the $C_5^3 \sin 3\theta$ residual term (top left) and its modal projection (top right) and the error between the two spaces (bottom).

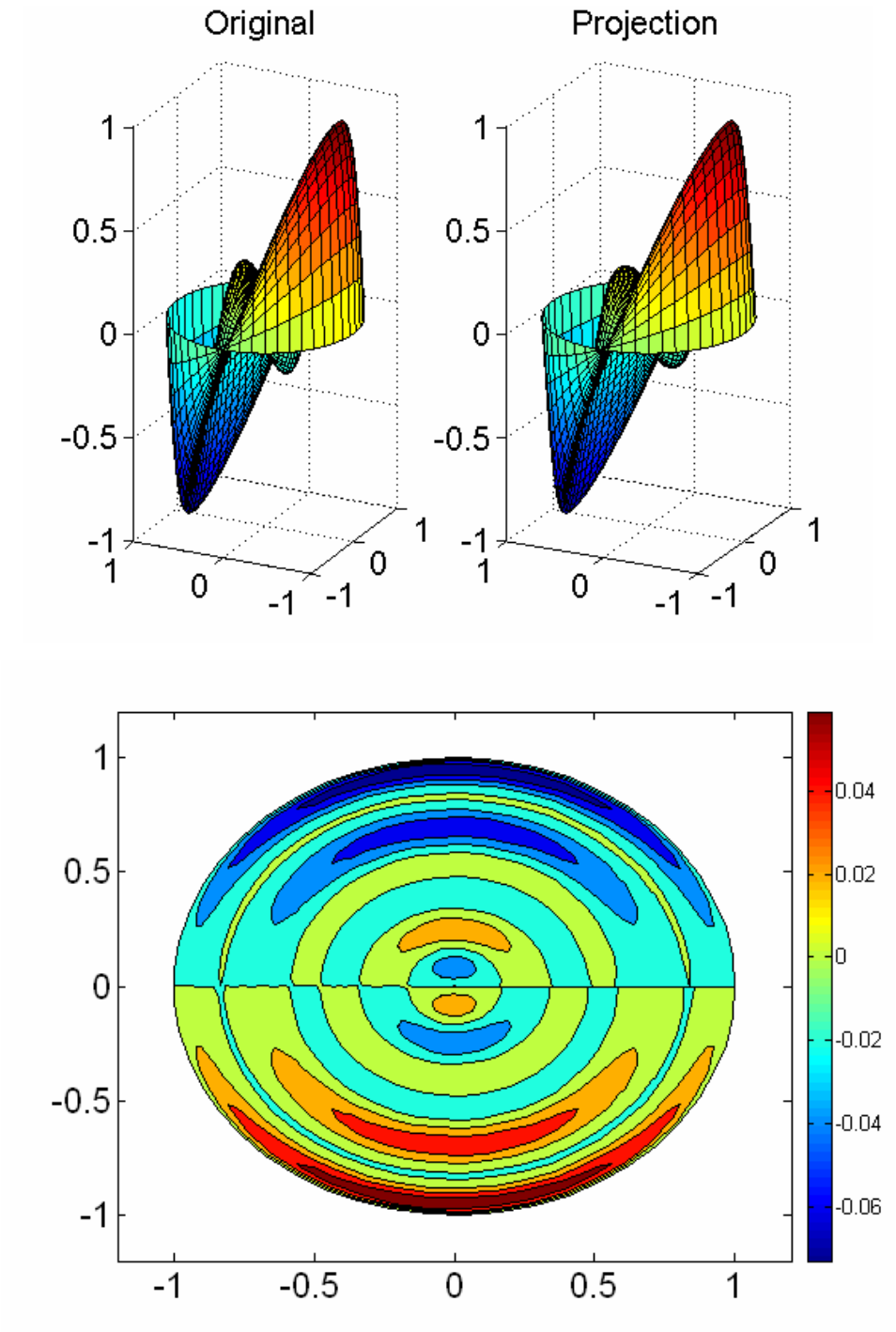

Figure 8.10. Comparison between the $C_5^1 \sin\theta$ residual term (top left) and its modal projection (top right) and the error between the two spaces (bottom).

Figures 8.6 – 8.10 demonstrate a useful mapping between the optical and mechanical worlds. By transforming a known incoming image aberration into two parts, a portion that can be corrected using uniform actuation pressure on the backside of the membrane lens and a portion that can be corrected using a distributed actuation pressure, we have shown that the deformable face of a membrane mirror can be used as a nearly 100% effective optic. The novel clamped Zernike radial polynomials provide a means for translating the incoming aberration into the two mentioned portions while simultaneously describing the necessary pressure distribution and magnitude for effective adaptive optic control. A proposed control scheme will be discussed in the future works section of the next chapter.

8.6 Chapter Summary

In the present chapter, we have developed a novel basis for conversing between the optical and mechanical worlds. The analysis performed has demonstrated that the structural characteristics of a circular membrane lens can be used advantageously as an advanced adaptive optic deformable mirror for eliminating nearly 100% of a 5^{th} order image aberration.

The proposed basis transformation has been described as the clamped Zernike radial polynomials. The clamped Zernike radial polynomials differ from traditional Zernike polynomials in that they have zero displacement at the boundary of the described image aberration. Consequently, the image aberration can be divided into two parts. The first portion of the aberration can be corrected by applying a uniform pressure on the backside of the membrane and via continuous deformation control of the boundary. The remaining residual portion requires a distributed actuation on the backside of the membrane. However, through the use of the clamped Zernike radial polynomials, the remaining residual is zero along the edge of the membrane—a conformable transformation to the structural configuration of the lens. Consequently, the distributed pressure necessary to eliminate the residual aberration can be easily transformed via a Fourier analysis into a modal summation based on the modes of a clamped circular membrane. Such a mapping

is key for describing the necessary form of actuation for making a 100% effective deformable membrane optic a reality in the near future.